Journal of Thermal Analysis and Calorimetry, Vol. 95 (2009) 3, 903–915

THE EFFECT OF PHYSICAL STATE ON THE DRUG DISSOLUTION RATE
Miscibility studies of Nimodipine with PVP

G. Z. Papageorgiou[1], *A. Docoslis*[2], *M. Georgarakis*[3] *and D. Bikiaris*[1*]

[1]Laboratory of Organic Chemical Technology, Department of Chemistry, Aristotle University of Thessaloniki 541 24 Thessaloniki, Greece
[2]Department of Chemical Engineering, Queen's University at Kingston, Kingston, ON K7L 3N6, Canada
[3]Section of Pharmaceutics and Drug Control, Department of Pharmacy, Aristotle University of Thessaloniki 541 24 Thessaloniki, Greece

In this work, the enhancement of drug dissolution rate through the preparation of new formulations containing Nimodipine in molecular level dispersion or in nanodispersion into poly(vinyl pyrrolidone) (PVP) matrix, was investigated. Differential scanning calorimetry (DSC) and modulated-temperature differential scanning calorimetry (MTDSC) in combination with X-ray powder diffractometry (XRPD) and scanning electron microscopy (SEM) studies showed that Nimodipine was amorphous in solid dispersions of 10 or 20 mass%, and mainly dispersed on a molecular level. This behaviour is attributed to the strong interactions taking place between the amine group of Nimodipine and carbonyl group of PVP. At higher drug loadings, crystal reflections in XRPD patterns and melting peaks of Nimodipine in DSC traces, indicated presence of drug in crystalline form. Micro-Raman studies in combination with SEM micrographs showed that the mean particle size increases with drug content in the formulations, up to 10 μm. Moreover, both XRPD patterns and micro-Raman spectra seem to indicate that Nimodipine crystallized in a second, thermodynamically stable, crystal modification II. The physicochemical characteristics of Nimodipine and the particle size distribution directly affect the dissolution rate enhancement, which is higher in amorphous dispersions.

Keywords: *dissolution enhancement, nanodispersions, Nimodipine, PVP*

Introduction

Nimodipine is a drug substance of the 1,4-dihydropyridene type which is used for the prevention and treatment of ischaemic neurological deficits caused by spasm of cerebral vessels following subarachnoid haemorrhage [1, 2]. Nimodipine is a chiral molecule and shows two polymorphic forms [3, 4]. Crystal modification I of Nimodipine refers to the racemic compound, while modification II to the conglomerate. Modification II is the thermodynamically stable form of the drug. Despite the fact that it is a highly permeable drug, Nimodipine exhibits low bioavailability after oral administration due to its slow dissolution in the gastrointestinal fluids (class II of the BCS), which represents the rate limiting step in the drug's absorption [5]. Detailed investigation of the solidstate of the drug is required prior to developing new formulations of Nimodipine. Unfortunately, in most cases recrystallization of Nimodipine cannot be prevented and so polymorphism must be also studied [3–6]. The improvement of its dissolution characteristics from its oral solid dosage forms is an important consideration towards enhancing its bioavailability and therapeutic efficiency.

Solid dispersions are defined as dosage forms whereby the drug is dispersed in a biologically inert matrix. Usage of solid dispersions aims at increasing the dissolution rate of drugs with low aqueous solubility. The latter is determinant of the oral bioavailability of a drug. Optimization of the wetting characteristics of the compound surface as well as increasing the interfacial area available for drug dissolution, facilitate higher drug dissolution rates from a solid dispersion [7]. Although increased interfacial area for drug dissolution can be easily accomplished by, for example, decreasing the particle size of the drug powder, micronized powders may result in further complications as they occasionally tend to agglomerate. A more preferable solution would be to introduce the drug in the form of a molecular dispersion [8].

The solid dispersion manufacturing process is crucial for the dissolution characteristics of the drug [9, 10]. Changes in solid-state of the active ingredient may alter its dissolution characteristics. Thus the preparation and storage conditions of solid dispersions are important [11–16]. Powder X-ray diffractometry (XRPD), differential scanning calorimetry (DSC), differential thermoanalysis, solution calorimetry, infrared spectroscopy and FT-Raman spec-

* Author for correspondence: dbic@chem.auth.gr

1388–6150/$20.00

Akadémiai Kiadó, Budapest, Hungary
Springer, Dordrecht, The Netherlands

troscopy are used for monitoring the stability of the amorphous state of the drug dispersed in the polymer [17–20]. Raman spectroscopy is a new powerful tool for the characterization of pharmaceutics [21–25].

Todate, there are only limited published works on solid dispersions of Nimodipine, most of them on using PEG as drug carrier [26–32]. In this work, solid dispersions of Nimodipine in poly(vinyl pyrrolidone) were prepared in order to increase its solubility. PVP is an amorphous polymer, and in contrast to PEG, it has been proved to form amorphous drug dispersions, which in turn favour enhancement of drug dissolution rates. The physicochemical characteristics of the above solid dispersions were studied in order to extract information about the transformation of the drug to the amorphous state and the crystalline polymorphic forms in comparison with the pure drug characteristics. Furthermore, the effect of the physicochemical characteristics and mainly the particle size distribution on the dissolution rates improvement was evaluated.

Experimental

Materials

Micronized Nimodipine (Nimo) with an assay of 101.2%, melting point of 125–128°C, aqueous solubility of approximately 0.5 mg L^{-1} and freely soluble in ethanol, was supplied from UQUIFA (Spain). The particle size distribution was determined using a Malvern Mastersizer S (633 nm) and found to range from about 1 μm (or less) to 29 μm (10% up to 1 μm, 50% between 1 and 9 μm, and 40% between 9 and 29 μm). Poly(vinyl pyrrolidone) (PVP) type Kollidon K30 with a molecular mass of 50,000–55,000 was purchased from BASF (Ludwigshafen, Germany). Ethanol absolute was purchased from Merck.

Preparation of solid dispersions

To prepare solid dispersions, the solvent evaporation method was followed using ethanol as the common solvent. Proper volumes of two solutions (5 mass%), one of the drug and one of the polymer (PVP), in ethanol were mixed and the mixture was ultrasonicated for 10 min. The solvent was removed by evaporation under vacuum in a rotary evaporator at 50°C for 24 h. Thus, solid dispersions with Nimo/PVP 10/90, 20/80, 30/70, 40/60 and 50/50 mass ratio were prepared. After complete removal of the solvent the samples were stored at 25°C in a desiccator.

Methods

Differential scanning calorimetry (DSC)

DSC study was performed on a Perkin-Elmer Pyris 1 DSC, equipped with Intracooler 2P cooling accessory. Accurately weighed samples (5 mg) were placed in standard aluminium pans and sealed with a lid. Heating rates of 20°C min^{-1} were applied with a nitrogen purge of 20 mL min^{-1}. Also, Modulated-Temperature DSC (MTDSC) study was performed using the same instrument used for standard DSC analysis. The Step-Scan Software of Perkin-Elmer was used. Step-Scan DSC is a temperature modulated DSC technique that operates, in conjunction with the power compensation DSC. The approach applies a series of short interval heating and isothermal steps to cover the temperature range of interest. With the Step Scan DSC approach, two signals are obtained. Thermodynamic C_p signal represents the reversible changes in the material, while the isothermal signal reflects the irreversible phenomena during heating. Because the sample is either heated or held isothermally (true isothermal), the Step Scan DSC approach is straightforward. In this study heating steps of 4°C at a heating rate 10°C min^{-1} between isothermal steps of 0.4 min were selected. Thus, scans from –50 to 220°C were performed and the average heating rate was 5°C min^{-1}.

X-ray powder diffractometry (XRPD)

XRPD study was performed over the range 2θ from 5 to 60°, at steps of 0.05° and counting time of 5 s, using a Philips PW1710 powder diffractometer, with CuKα Nickel-filtered radiation.

Scanning electron microscopy (SEM)

The morphology of the prepared solid dispersions as well as the physical mixtures was examined by a scanning electron microscopy system (SEM) Jeol (JMS 840). The films were covered with carbon coating in order to increase conductivity of the electron beam. Operating conditions were accelerating voltage 20 KV, probe current 45 nA and counting time 60 s.

Fourier transform infrared spectroscopy (FTIR)

FTIR spectra were obtained using a Perkin Elmer FTIR spectrometer, model spectrum 1000. In order to collect the spectra, a small amount of each material was used by compression in KBr tablets. The IR spectra were obtained in the spectral region 400–4000 cm^{-1} using resolution 4 cm^{-1} and 10 co-added scans.

Micro-Raman spectroscopy

Raman studies on Nimodipine formulations were performed by using a Horiba/Jobin- Yvon microRaman Spectrometer (Model: LabRAM) with spectrum resolution capability 2–3 cm^{-1}, equipped with a 632 nm He/Ne laser source, 1800 1 nm^{-1} grating and an Olympus BX41 microscope system. Collection of the spectra was performed in backscattering mode at room temperature under the following conditions: ×100 microscope objective, 100 μm pinhole size, 300 μm slit width, and 20 s exposure time. Each spectrum represents the average of two measurements. Sample profiling (2D mapping) was performed under the same conditions at a step increment of 0.5 μm in both *x*- and *y*-direction.

Dissolution testing

The test was performed at 37°C and 100 rpm. 1000 mL of aqueous solution containing 0.5% (mass/mass) of Sodium Lauryl Sulphate was used, in order to identify potential differences in the dissolution profile of the examined preparations. Samples were collected at 10, 20, 30, 45, 60, 90, 120, 180, 240 and 300 min using an automatic sampler type Distek Evolution 4300 and analyzed immediately after sampling, according to an appropriately validated UV method, at 353 nm, using a UV-Vis spectrophotometer type Shimadzu 1601. Nimo/PVP systems of 10/90, 20/80, 30/70, 40/60 and 50/50 mass/mass prepared by the solvent evaporation methods, as well as a physical mixture of Nimo/PVP 10/90 and 50/50 mass/mass were evaluated. The test was performed in triplicate while the RSD was found to be less than 3%.

Results and discussion

Characterization of the solid dispersions

Despite the fact that all Nimodipine/PVP solid dispersions were prepared by solvent evaporation under the same conditions, the visual appearance of the final samples showed a significant variation with drug content. Since PVP is amorphous, the observed variations have to be linked directly to differences in the drug's physical structure in those mixture. Specifically, the solid dispersions having a drug content of 20 mass% or less were glassy-transparent with a light yellow colour, showing that the drug was most probably in the amorphous state. The solid dispersions containing higher than 30 mass% Nimodipine were opaque with a white colour, maybe due to the drug crystallization.

To detect the solidstate of the dispersions XRPD patterns of the samples were recorded after a short period of storage (ten days) in comparison with their respective physical mixtures. The XRPD patterns of the solid dispersions are shown in Fig. 1a. The patterns corresponding to physical mixtures showed crystallinity of the drug for all mixing ratios (data not shown). On the other hand, the solid dispersions at 10 or 20 mass% Nimodipine concentrations did not show crystalline reflections. Only the two amorphous halos of PVP were present in the XRPD patterns [33]. It seems that PVP is an effective carrier for the preparation of amorphous dispersions at low drug concentrations [34, 35] while this is not possible to achieve when crystalline carrier like PEG are used as carriers [36, 37]. However, at higher drug concentrations the drug recrystallized.

Another important point that emerged from the examination of the XRPD patterns is the type of crystal modification. More specifically, the crystalline peaks in the XRPD patterns of the Nimo/PVP 30/70 up to 50/50 mass/mass solid dispersions were found to be consistent with the crystalline reflections of the known crystal modification II of Nimodipine [3, 4, 38]. In the patterns for the respective physical mixtures, crystal reflections of modification I were observed, same as those for the original Nimodipine sample used for the preparation of both the physical mixtures and solid dispersions. Moreover, results from a separate study we conducted show that recrystallization of the drug to modification II crystals was also observed in the case of the Nimo/PEG solid dispersions prepared also by solvent evaporation [24]. The above XRPD study of the solid dispersions was repeated after six months and finally the samples were tested after two years. There were no differences between the patterns for the solid dispersions despite the long storage, meaning that neither increase was observed in the drug crystallinity nor transition of crystal modification was detected (Fig. 1b). This finding is in agreement with a recent study by Urbanetz who found that PVP prevents the recrystallization of Nimodipine and thus stabilizes its physical state during storage [25].

An indication of the physical state and degree of miscibility for the prepared Nimodipine/PVP solid dispersions can be obtained by means of DSC analysis [39–42]. The DSC traces conducted on solid dispersions with 10 and 20 mass% drug content showed no melting peak for Nimodipine (Fig. 2), in agreement with the XRPD patterns. However, melting of the drug was observed in the solid dispersions containing higher amounts of drug. Grunenberg *et al.* in their paper on the polymorphism of Nimodipine used the onset temperature of the melting peak as the melting temperature of the crystals [3]. Thus, it was reported that the T_m for modification I crystals is 124°C,

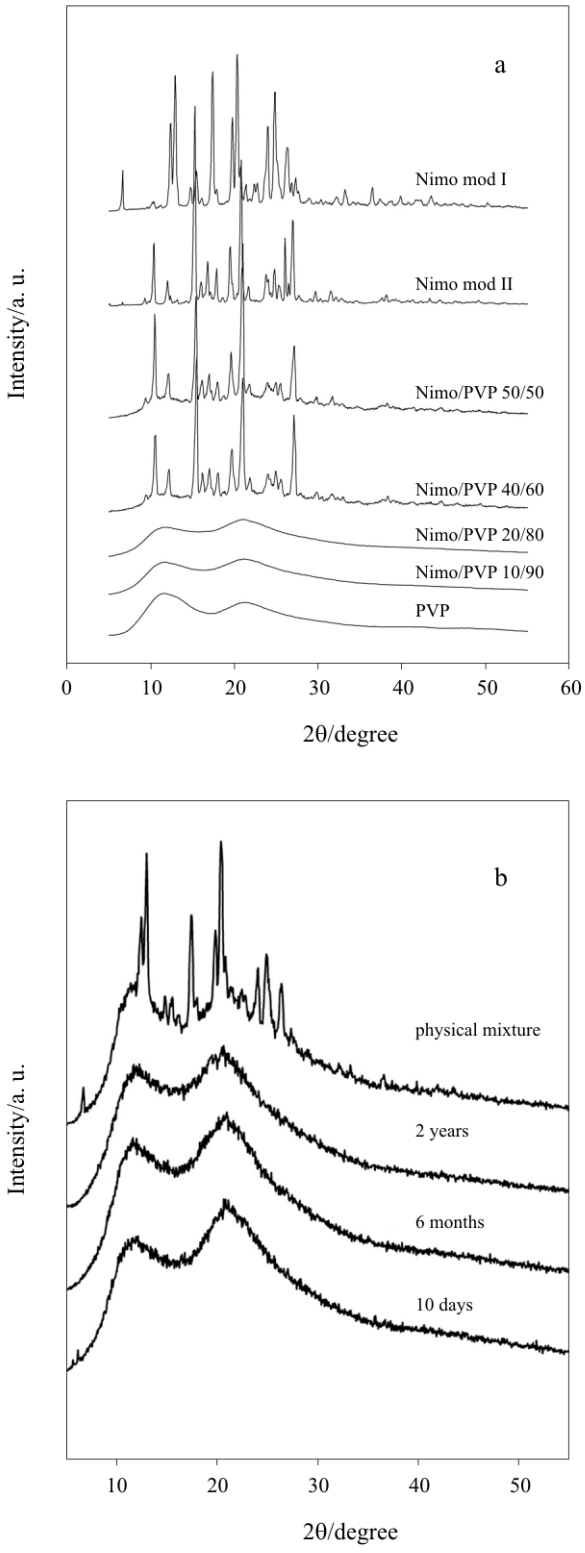

Fig. 1 a – XRPD patterns of Nimodipine/PVP solid dispersions, b – XRPD patterns of Nimodipine/PVP 20/80 mass/mass solid dispersion after different storage times

while modification II crystals have a T_m of 114°C. In the case of Nimo/PVP solid dispersions with high drug load, melting begins at lower temperature, which rather shows presence of Nimodipine modification II crystals, in contrast to the physical mixtures for which the higher melting temperature is consistent with Nimodipine crystal modification I. It should also be noted that the glass transition temperature (T_g) of Nimodipine was in the region of 20°C, as tests of amorphous (melt-quenched) samples showed (data not shown here for briefness). This low T_g value means that Nimodipine may crystallize during storage at room temperature [43–45].

In order to acquire more accurate data on the thermal behaviour and physical state of the prepared solid dispersions, Step-Scan MTDSC was employed. The recorded curves showed that the Nimo/PVP 10/90 and 20/80 mass/mass solid dispersions exhibit single composition dependent T_g, as one can see in Fig. 3a. The T_g value of pure PVP was found to be 161°C while for Nimodipine 20°C. The T_g of the solid dispersions decreased with increasing Nimodipine content, to 130 and 105°C for the 10/90 and 20/80 mass/mass solid dispersions, respectively. As can be seen, by using the Step-Scan MTDSC the T_g of each solid dispersion is recorded with higher ac-

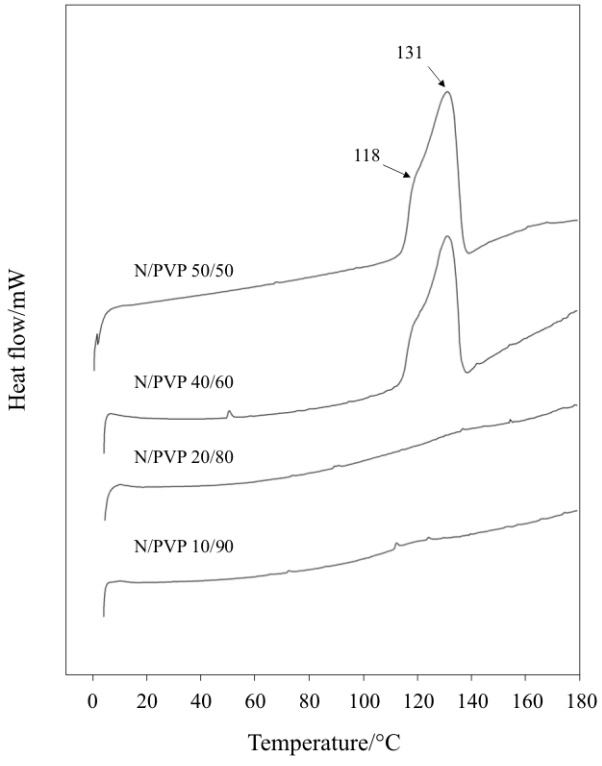

Fig. 2 DSC traces of Nimodipine/PVP solid dispersions after 6 months

curacy and is more pronounced (Fig. 3b). From these curves it seems that Nimodipine and PVP were miscible at low Nimodipine content. Systems exhibiting a single T_g are believed to be either single-phase mixtures where the drug exists in molecular level dispersion or mixtures where the minor component is dispersed in the form of particles of less than 10–20 nm in diameter into the matrix of the component in excess [37, 46]. However, in studied solid dispersions containing higher Nimodipine load (30–50 mass%), two melting points of Nimodipine are recorded. The first one at 118°C, which is attributed to the crystal mod II and a second one at 131°C attributed to the crystal mod I. The magnitude of the second peak is much higher indicating that Nimodipine is mainly in the crystal mod I. However, from XRPD it was found that in these solid dispersions Nimodipine is in mod II (Fig. 1). So it seems that during DSC scans the mod II is melted and immediately transforms to the crystal mod I, which is thermodynamically more stable. After quenching and subsequent heating of these solid dispersions the melting point of Nimodipine is disappeared and two glass transitions were recorded, close

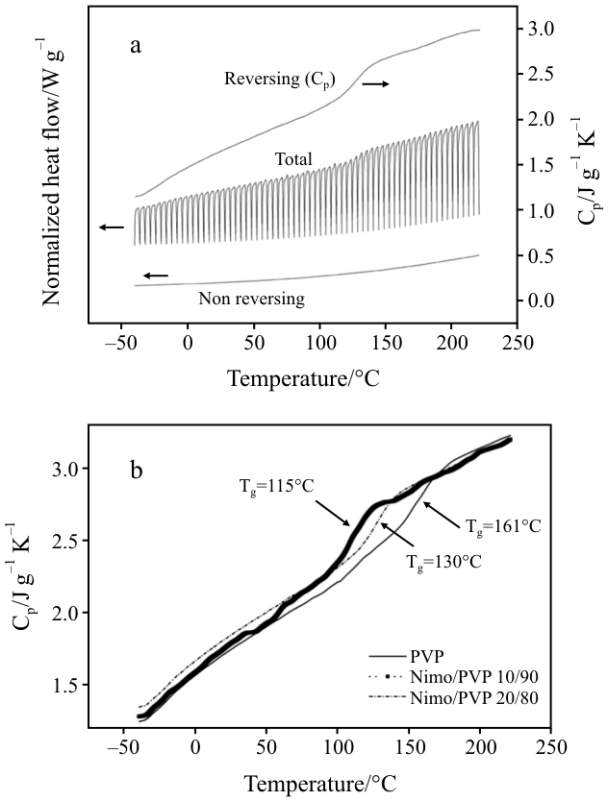

Fig. 3 Step-Scan MTDSC data a – Reversing signal (C_p), total and non-reversing signal (isothermal baseline) for the Nimo/PVP 10/90 mass/mass solid dispersion obtained by heating rate at 5°C min^{-1}; b – Reversing signal (C_p) for the pure PVP, Nimo/PVP 10/90 and 20/80 mass/mass solid dispersions

to T_gs of the initial components. The latter indicates that the PVP and Nimodipine are both in amorphous state, but were separated. As a matter of fact, the T_gs of both components are slightly shifted to intermediate values, which indicates some limited miscibility, caused by interactions between the drug molecules and polymer chains.

Several theoretical and empirical equations have been proposed for miscible systems with the purpose to estimate the extent of interactions between the mixture components and also correlate their glass transition temperatures to the mass fractions and glass transitions of the pure components. Among them, the Fox equation can be used to capture the T_g/composition relationship [47]:

$$1/T_g=w_1/T_{g_1}+w_2/T_{g_2} \quad (1)$$

where, T_g is the glass transition temperature of the blend, w_1 and w_2 are the overall mass fractions of the two components forming the blend and T_{g_1}, T_{g_2} are their glass transition temperatures. By using the Fox equation the T_g of the solid dispersions containing 10 and 20 mass% Nimodipine, which show a single glass transition and thus are completely miscible, is predicted to be 94.4 and 66.8°C, respectively. However, these values are very low and far away from those recorded by DSC. This large difference between the predicted and recorded temperatures is an indication that strong interactions are taking place between the two components. For this case, Gordon and Taylor proposed an equation that captures the effect of interactions that are not accounted for by the Fox equation [48]:

$$T_g=(w_1T_{g_1}+kw_2T_{g_2})/(w_1+kw_2) \quad (2)$$

where k is a constant representing a semi-quantitative measure of the interaction strength between the functional groups. If k takes values close to 1 or higher then it is suggested that strong interactions take place, as for example, in the PVP/PVAL or polyglutarimide/poly(styrene-co-maleic anhydride) blends [49, 50]. However, as found in our previous study, miscible systems can be formed when these interactions are low, i.e., k takes values less than 1 [51]. By applying the measured T_gs into the Gordon–Taylor equation it was found that the values of k are 2.53 and 2.49 for the solid dispersions containing 10 and 20 mass% Nimodipine, respectively. These values are much higher than 1, implying that indeed the interactions between the functional groups of Nimodipine and PVP are very strong.

In solid dispersions containing higher than 30 mass% Nimodipine, which appear to have two shifted glass transitions at different temperatures than the initial components, this shift is caused by interactions taking place between the components. More-

over, the shifts may be also the result of the penetration of each component into the phase primarily composed of the other. The amount of each component contained in the two phases can be calculated using the empirical equation of Fox, by taking into account the T_g shifts [47]:

$$w_1' = (T_{g_{1b}} - T_{g_2})/(T_{g_1} - T_{g_2}) \quad (3)$$

where w_1' is the apparent mass fraction of the substance 1 in that substance's rich phase and $T_{g_{1b}}$ is the observed T_g of the substance 1 in the blend. The same equation can be applied to calculate the apparent mass fraction of the second component w_2' in the other phase. By using Eq. (3) and the T_g values measured with DSC, the apparent volumes of each component in the two phases of the Nimo/PVP mixture were calculated. The results are summarized in Table 1.

As shown in Table 1, by increasing the amount of the polymer in the system, the mass fraction of PVP in the Nimodipine-rich phase and mass fraction of Nimodipine in the PVP-rich phase also increases. This behaviour leads to partial miscibility between PVP and Nimodipine in the glassy state and for this reason the recorded T_gs are shifted to different temperatures, compared with the initial components. The presence of the PVP macromolecules in the Nimodipine-rich phase, as well as the presence of Nimodipine into PVP phase, could be explained with the interactions that take place between the reactive groups.

FTIR analysis

It is important to note that Nimodipine has an amine group in its molecule, which is able to form hydrogen bond with the carbonyl groups of the PVP macromolecules. The assumption that interactions between unlike molecules can lead to partial miscibility of the Nimodipine-PVP mixtures was investigated by using FTIR spectroscopy. Figure 4 shows the IR spectra of pure Nimodipine (crystal form I), after recrystallization from ethanol solution (crystal form II), prepared by melt quenching (amorphous), as well as the spectra of the solid dispersions. As can be seen there are differences in the spectra of the different modifications of Nimodipine. Thus, the spectra of solid dispersions should rather be compared with those of the Nimodipine modification occurring in the specific samples. In the spectra for the Nimo/PVP 10/90 and 20/80 mass/mass solid dispersions, in which Nimodipine was amorphous, a shift was found in the peak corresponding to the absorbance of –NH– of amorphous Nimodipine to lower values. Specifically the peak in the pure drug spectrum was at 3335 cm^{-1} while it was observed at 3290 and 3270 cm^{-1} in the spectra of the Nimo/PVP 10/90 and 20/80 mass/mass solid dispersions, respectively. This is most probably a proof that hydrogen bonds are formed. Also, a shift was observed in the absorbance of carbonyl group of PVP from 1662 for the pure polymer to 1658 and 1653 cm^{-1} in the spectra for the 10/90 and 20/80 mass/mass solid dispersions, respectively. The above verified the presence of interactions promoting amorphization of the drug (Fig. 4c). Similar interactions were reported to occur between the amide group of Felodipine (a drug of the same family as Nimodipine) and PVP carbonyl groups, which result in amorphisation of Felodipine in its solid dispersions with PVP, as well as dissolution rate enhancement [52].

From these spectra it is obvious that the involved interactions are higher in the sample containing 20 mass% Nimodipine since the corresponding wavenumbers are shifted to much lower values compared to the sample containing 10 mass% Nimodipine. However, in the solid dispersions containing higher than 30 mass% Nimodipine the corresponding wavenumbers of Nimodipine are shifted by only 2–5 cm^{-1} at lower positions, indicating that the interactions are of lesser magnitude (Fig. 4b). This is because the solid solution became progressively saturated and Nimodipine crystallizes creating a two-phase system.

Micro-Raman

The spatial distribution of Nimodipine, the amorphous content and its polymorphism in the case that

Table 1 Apparent mass fraction of Nimodipine (Nimo) and Poly(vinyl pyrrolidone) (PVP) in the rich phase of each component

			NIMO Rich Phase		PVP Rich Phase	
Ratio of Nimo/PVP (mass/mass)	T_g Nimo/ °C	T_g PVP/ °C	w_1' of Nimo	w_2' of PVP	w_1'' of Nimo	w_2'' of PVP
100/0	20.0	–	–	–	–	–
30/70	42	137	0.844	0.156	0.170	0.830
40/60	37	148	0.880	0.120	0.092	0.908
50/50	26	156	0.957	0.043	0.050	0.950
0/100	–	161	–	–	–	–

crystalline drug occurred in the solid dispersions, were also studied by means of micro-Raman spectroscopy and SEM. Our previous study demonstrated that these techniques can be successful in the examination of a drug's particle size distribution inside a polymer matrix [53]. However, since Nimodipine creates different crystal forms, its polymorphism should first be examined. The two modifications of Nimodipine exhibit different Raman and IR spectra [3]. In the present study, their identification by Raman spectroscopy became possible by using as criterion the intensities of the peaks observed at 1347 and 1642 cm^{-1}. In a Raman spectrum, the intensity ratio I_{1347}/I_{1642} is greater than unity for Mod I (racemic compound) and the opposite is true for Mod II (conglomerate). Moreover, this ratio varies greatly not only between different crystal modifications but also between the crystalline and amorphous state of the drug in its pure form and thus it can be used to determine the physical state of the drug. This is demonstrated in Fig. 5, where typical Raman spectra for these three distinct cases, two crystalline and the amorphous state are shown.

As seen in Fig. 5, when the drug crystallizes in Mod I, the band assignment at 1642 cm^{-1} is significantly suppressed and this results in an intensity ratio much larger than one. On the other hand, when the

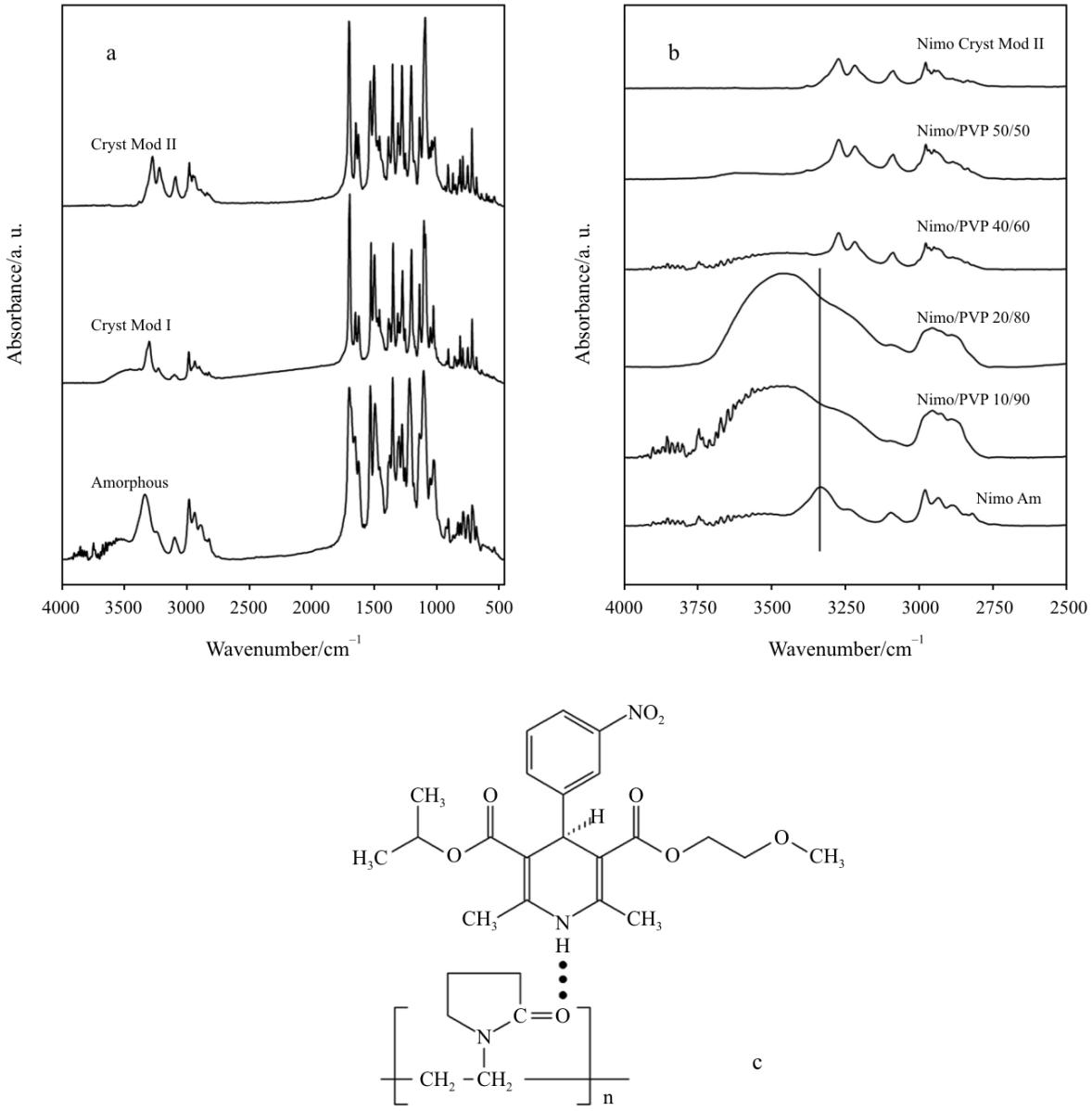

Fig. 4 a – FTIR spectra of amorphous and crystalline Nimodipine (mod I and mod II); b – FTIR spectra of the Nimo/PVP solid dispersions compared to those of pure Nimodipine and c – schematic representation of the hydrogen bonds between the Nimodipine and PVP molecules

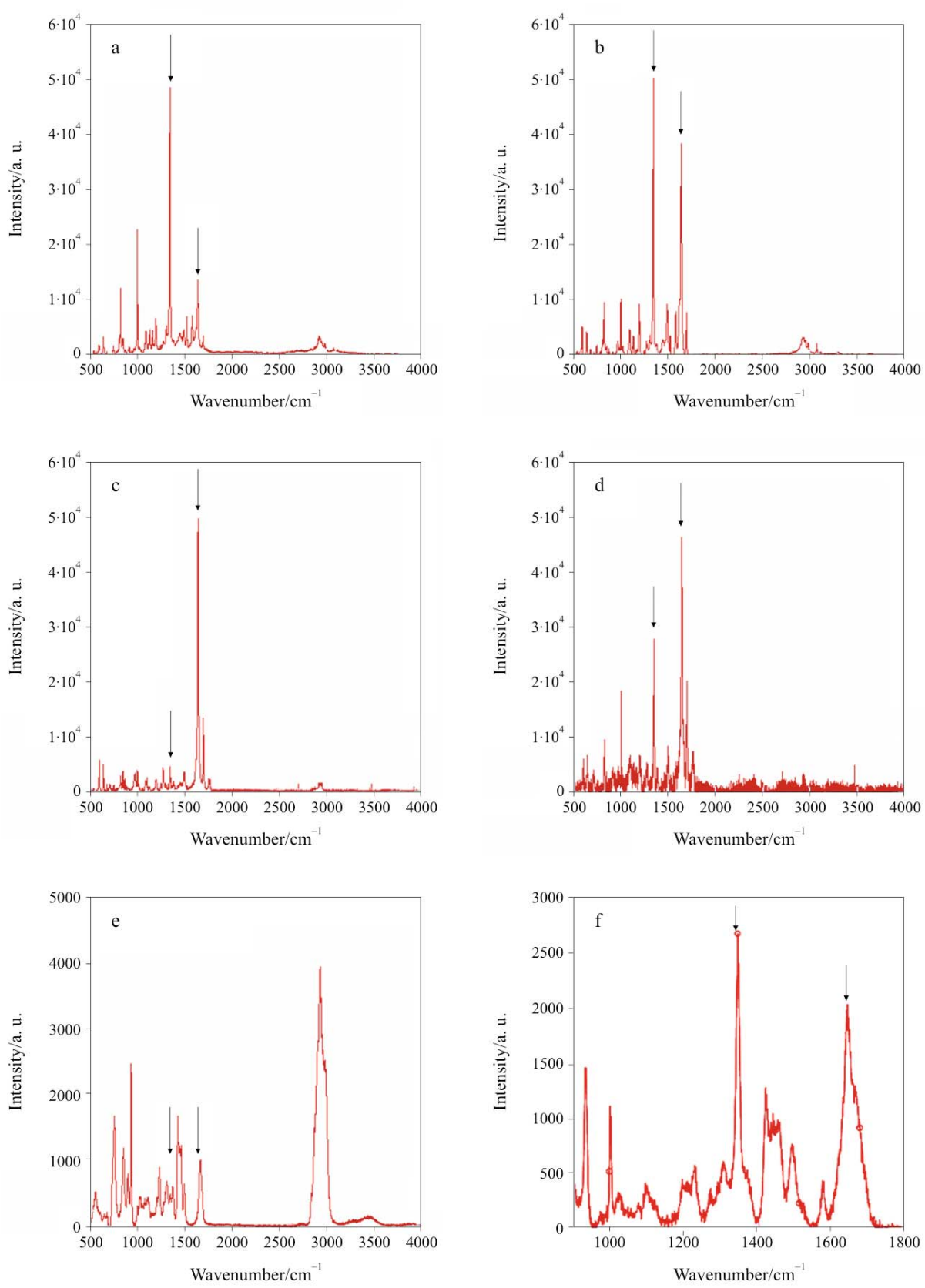

Fig. 5 Raman spectra of Nimodipine existing in different forms: a – crystal of Mod I; b – amorphous phase I; c – crystal of Mod II; d – Amorphous phase II; The polymorphs can be distinguished on the basis of the peak intensities at 1347 and 1642 cm^{-1} (indicated by the arrows); e – Raman spectrum of pure PVP; f – Detail from a Raman spectrum corresponding to Nimo/PVP 10/90 mass/mass solid dispersion

drug crystallizes as Mod II, the band assignment at 1347 cm^{-1} almost disappears. Thus, the resulting intensity ratio now becomes much smaller than unity. Finally, the intensity ratio for the amorphous drug is found to lie between those two values. The variation of these intensity ratios as a function of the physical state of the pure drug is shown collectively in Table 2. The tabulated mean values correspond to one hundred measurements taken from each sample. Inspection of Table 2 reveals distinct differences in the values of the intensity ratios; hence the latter are being used here as means for determining the physical state and spatial distribution of the drug in its solid dispersions in PVP.

Examination of the Raman spectra of pure Nimodipine and PVP compounds (Fig. 5) shows that the two materials do not share major characteristic peaks; therefore, the contribution of each one of them in their respective mixtures could be easily identified. The only overlap seems to occur around the region that corresponds to the stretching vibrations of the carbonyl bond (>C=O). The maximum values of the corresponding peaks for Nimodipine and PVP are found at 1642 and 1662 cm^{-1}, respectively. Although the two peaks almost overlap in the mixtures, a distinction between them is always possible by virtue of the fact that the one corresponding to Nimodipine has a significantly higher intensity. An example of this can be seen in Fig. 5f, which displays a Raman spectrum obtained from a sample with 10 mass% drug content. Even at this low mixing ratio, the intensity of the peak at 1642 cm^{-1} (Nimodipine) is significantly higher, whereas that of PVP appears as a weaker 'shoulder' peak.

The size and spatial distribution of domains where Nimodipine existed as amorphous or crystalline forms was performed by means of micro-Raman mapping (XY scan) on randomly selected areas in a number of samples. Examples can be seen in Figs 6 and 7, where mapped areas corresponding to solid dispersions of Nimo/PVP with 10/90 (amorphous) and 40/60 mass/mass (crystalline) mixing ratios are shown. Unless otherwise specified, the colour bars (scale 0-4) indicate the value of the intensity ratio

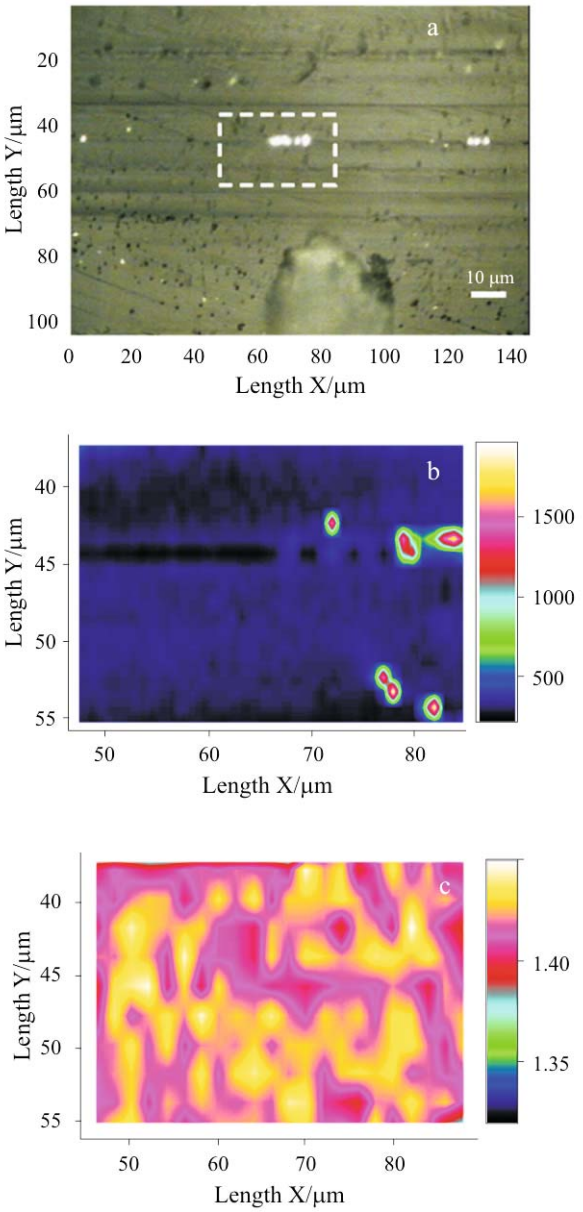

Fig. 6 MicroRaman XY scan of a sample area corresponding to the Nimo/PVP 10/90 mass/mass solid dispersion. a – Optical micrograph of the sampled area; b – Color intensity profile corresponding to the peak at 1347 cm^{-1}; c – Examination of the same area in terms of the peak ratio I_{1347}/I_{1642} shows that the drug exists everywhere in the amorphous phase

Table 2 Intensity ratios corresponding to the three types of Nimodipine found in this study. The columns labeled 'Peak 1' and 'Peak 2' indicate the wavenumber range over which peak intensity values were observed for these two-band assignments

Modification	Structure	Peak 1/cm^{-1}	Peak 2/cm^{-1}	Intensity ratio, R ($=I_1/I_2$)	
				Mean	S.D.
I	Crystalline	1347–1348	1642–1643	3.67	0.58
I	Amorphous	1348–1351	1645–1647	1.22	0.17
II	Amorphous	1347–1350	1645–1647	0.83	0.074
II	Crystalline	1347–1348	1643	0.171	0.035

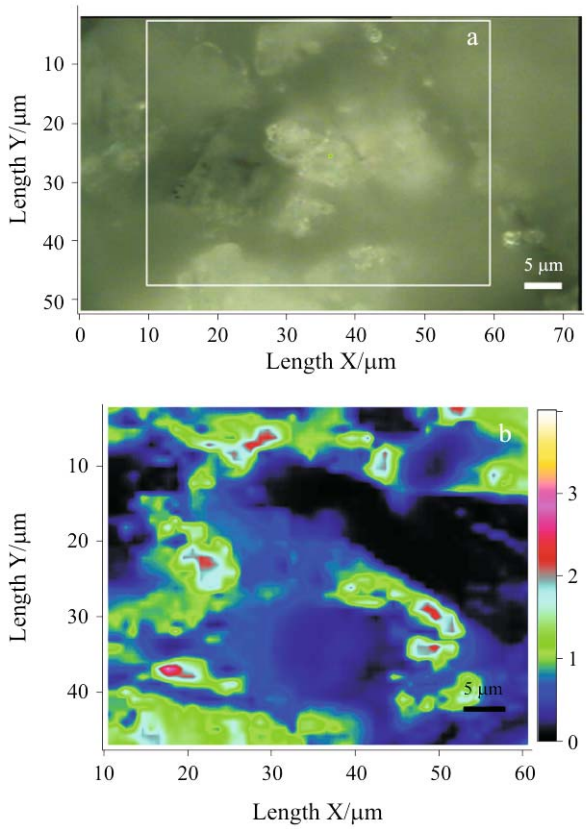

Fig. 7 a – light microscope and b – corresponding micro-Raman XY scan, images from a PVP/Nimo 40/60 mass/mass sample

I_{1347}/I_{1642} in the sample. Using as key the values from Table 2, dark blue domains correspond to crystals of Mod II while yellow domains correspond to crystals of Mod I. Values in between can be attributed to the amorphous phase of the drug.

Figure 6 shows the result of micro-Raman mapping of a sample area corresponding to the Nimo/PVP 10/90 mass/mass solid dispersion. Figure 6a shows the optical micrograph of the sampled area with the dashed square outlining the mapped area. The bright spots are surface contamination during preparation of the samples. In Fig. 6b, the colour intensity profile corresponding to the peak at 1347 cm^{-1} is shown. The blue areas (week signal) indicate uniform drug dispersion and also low drug content (10 mass%). The coloured spots observed in some areas of the images suggest domains of higher drug concentration. In Fig. 6c, a colour plot corresponding to the local values of the I_{1347}/I_{1642} intensity ratio is shown for the same area. Here all the areas appear to have almost the same value. According to Table 2, the value of the intensity ratio indicates drug existing everywhere in amorphous state. It is noteworthy that even in the areas where high local drug concentration was detected (red spots in Fig. 6b), the drug remains amorphous. Similar results were observed for the Nimo/PVP 20/80 mass/mass solid dispersion. Overall, it can be inferred that at drug concentrations below the saturation point in PVP, Nimodipine exists in fine dispersion and in amorphous state. Domains with dimensions 1–2 μm inside which the drug exists at higher than average concentrations where also detected, however their number is limited and probably accounts for a very small portion of the drug. From the above, and given that the mapping resolution here is on the order of 0.5 μm, we can assume that the drug mainly exists in a state of molecular level dispersion and/or in the form of nanoparticles dispersed in the PVP matrix.

On the other hand, micro-Raman mapping performed on samples of higher Nimodipine content (above the saturation concentration) showed a less homogenous dispersion of the drug. Colour maps of randomly selected areas from samples with overall Nimodipine content equal to 40 mass% is shown in Fig. 7. The light microscope image was taken with a ×100 magnification lens. The color map represents the spatial variation of the ratio I_{1347}/I_{1642} within the area indicated by the white square in the optical image. In this sample, extended areas characterized by higher-than-average drug concentration appear everywhere, indicating drug recrystallization with crystal sizes up to 5 and 10 μm for the solid dispersions containing 40 mass% Nimodipine. This was in agreement with the XRPD and DSC observations that also detected crystalline domains. From this colour map becomes obvious that the vast majority of the drug that crystallized ended up forming Mod II crystals. However, these crystals are surrounded by large areas represented by an intensity ratio in the range $0.25<I_{1347}/I_{1642}<3.5$, which cannot be readily classified as corresponding to completely crystalline (Mod I or Mod II) or amorphous nimodipine (Table 2). Detailed examination, involving observations of the location and intensity of characteristic peaks within each spectrum, of a large number of spectra obtained from those areas and their comparison against those received from pure Nimodipine (Fig. 4) showed that areas represented by a ratio $0.25<I_{1347}/I_{1642}<3.5$ correspond to domains where Nimodipine co-exists with PVP, however it can be present simultaneously in more than one forms (e.g, amorphous and crystalline). Moreover, from the spectra it was observed that the composition of nimodipine in those areas varies significantly with location. Therefore these areas can be best described as heterogeneous. Identification of individual domains within those areas where nimodipine existed only in a single form could not be performed, as the size of these domains was below the resolution capabilities of the instrument (i.e., <100–500 nm) used in this study.

Therefore, we can only speculate that these areas contained crystals of Nimodipine of molecular to submicron-sized dimensions and/or amorphous regions formed in the presence of PVP. Detailed analysis of the Raman spectra, e.g., through peak de-convolution and subsequent integration of the area under each Raman peak, can possibly provide more information on the composition and amounts of Nimodipine present in each domain, however this analysis is usually cumbersome and time-consuming.

Due to the extended dispersion of these particles into PVP matrix it can be inferred that Nimodipine exists in molecular dispersion in these areas. It is known that the amorphous glassy state shows some short-range order. The difference with the crystalline state is that in the latter there also exists a long-range order. Nimodipine is in fact a racemic mixture that is a 50/50 mass/mass mixture of the two optical antipodes. It would be reasonable to assume that at room temperature the drug antipodes, if not in the crystalline state but in the glassy state, may be uniformly mixed as in the racemic liquid or they may be segregated to some extent. As it was reported above, crystallization in the form of a conglomerate (i.e., Mod II crystals) means that the two antipodes crystallize separately.

In an attempt to assess the amount of each modification in the samples, Raman spectra were collected randomly from samples with surface area of approximately 1 cm^2. A total of 100-point measurements were taken from each sample. The state of the drug at the point of measurement was determined from the value of the I_{1347}/I_{1642} intensity ratio of the corresponding Raman spectrum. The data are shown in Table 3. Because of the relatively small number of point measurements per sample, the tabulated results can serve only as indications of the approximate distribution of each modification in the samples. The results, however, are in qualitative agreement with those obtained from Raman mapping and XRPD. It should be noted here that for 10 or 20 mass% Nimodipine content in the solid dispersions, the drug practically appears to be completely amorphous, while the amount of measurements that showed crystalline areas is negligible (3–4%). This finding is consistent with the hypothesis regarding the extent of interactions between the different solid dispersions. These limited crystalline amounts of Nimodipine in the particular solid dispersions are not possible to be detected with XRD and DSC and can explain why the interaction parameters calculated with DSC are lower in the case of solid dispersion containing 20 mass% Nimodipine. As expected, the degree of crystallinity of Nimodipine increased with drug content in the solid dispersions, reaching a 72% for the Nimo/PVP 50/50 mass/mass sample.

Scanning electron microscopy study

In order to verify the above recorded results, all solid dispersions were subjected to SEM examinations. The results from the SEM study showed that the Nimo/PVP solid dispersions with 10 or 20 mass% drug load did not contain drug crystals. Occasionally, only very small Nimodipine particles were observed and these did not show well-shaped prismatic or crystal-like features. In samples with 30 mass% and higher drug load, large Nimodipine particles could be seen (Fig. 8). These findings from SEM micrographs are in good agreement with the micro-Raman results, providing consistent indication of the particle size distribution of Nimodipine into PVP matrix as a function of concentration. It is well known that in order to increase the dissolution rate of a drug that is poorly soluble in water, its particle size must be lower than 1 μm [14]. It is therefore expected that the dissolution rate of Nimodipine from its solid dispersions would increase in cases where the drug exists as molecularly dispersed or in the form of nanoparticles.

Dissolution rates

The dissolution behavior of the solid dispersions and their physical mixtures was studied after their preparation as well as after six months, in order to find if there is any alteration caused by samples storage. As can be seen from Fig. 9 the dissolution rates of the

Table 3 Influence of drug content on the distribution of nimodipine in the solid dispersions. The tabulated results are based on 100 measurements per sample

Mixture	Solid dispersion			
Composition	Nimo/PVP 10/90 mass/mass	Nimo/PVP 80/20 mass/mass	Nimo/PVP/ 40/60 mass/mass	Nimo/PVP 50/50 mass/mass
Mod I, Crystal	2	0	8	5
Mod I, Amorphous	94	92	31	14
Mod II, Crystal	1	4	48	67
Mod II, Amorphous	3	4	13	14
Total (/100)	100	100	100	100

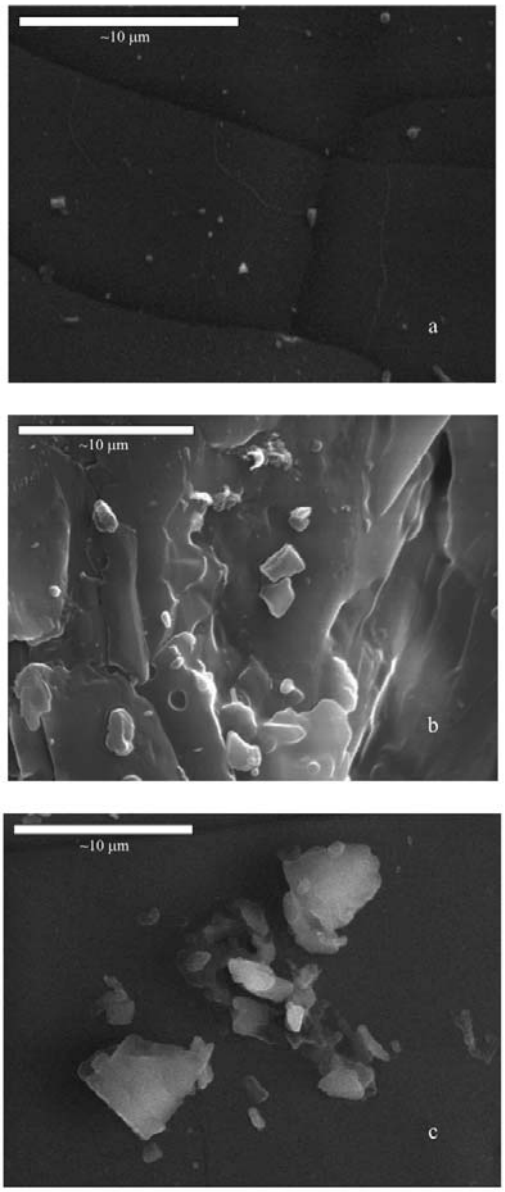

Fig. 8 SEM microphotographs for Nimo/PVP a – 20/80, b – 40/60, and c – 50/50 mass/mass

drug from its solid dispersions not only were higher with respect to the pure drug, but also showed up to 30-fold increase in the case of 50 mass% Nimodipine. Even for the physical mixture with 10 mass% Nimodipine, for which the initial rate of dissolution was comparable to those of the solid dispersions, the ultimate release value did not exceed 60-70%. An amount equal to the 85 and 65% of the total drug load was released within one hour from the solid dispersions containing 10 and 20 mass% Nimodipine, respectively, whereas total (100%) release was achieved within 3 h. For the solid dispersions with 30 mass% drug or more the drug release was both slower and limited. It seems that the crystalline drug can no more be dissolved. As it was reported above

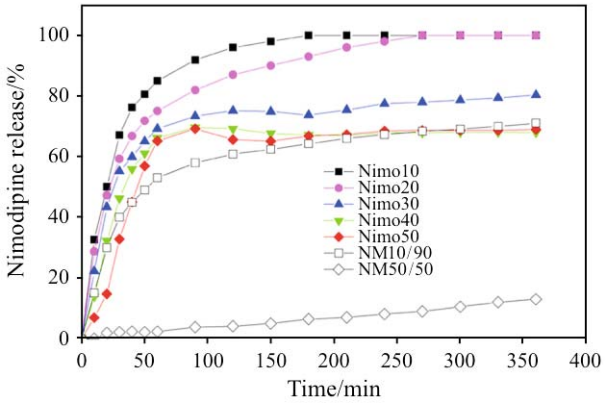

Fig. 9 Nimodipine release from Nimo/PVP solid dispersions and physical mixtures (the latter are indicated by NM10/90 and NM 50/50 mass/mass)

Nimodipine mod II crystals were formed in these solid dispersions. The decreased solubility of Mod II crystals probably plays its role in this case. After all, the drug amorphization due to fine dispersion in the polymer matrix, either as molecular dispersion or in the form of nanoparticles, obviously resulted in enhancement of the dissolution rates. The polymer-drug miscibility in the amorphous phase was crucial towards dissolution enhancement.

Conclusions

Solid structure of Nimodipine in PVP was studied in order to understand the relation between the physical state and resulting dissolution enhancement. XRPD showed that the drug was kept in the amorphous state in the samples containing up to 20 mass% Nimodipine. It seems that for low drug concentrations the drug is in a molecular dispersion or in the form of nanoparticles. On the other hand for higher drug content the solid dispersions turned to solid suspensions in which the excess Nimodipine amount recrystallized creating crystal particles with sizes up to 10 μm. XRPD, DSC and micro-Raman results showed formation of Mod II crystals of the drug. Micro-Raman mapping revealed that not only crystals of two different modifications could be observed, but also that the crystallization process affected the amorphous phase. In general high amorphous portions were observed for the drug in the solid dispersions. The dissolution study showed enhanced rates for the solid dispersions containing amorphous drug. When Nimodipine crystallized in Mod II crystals, the release was limited as a result of the decreased solubility of the Mod II drug crystals.

Acknowledgements

This work was funded by the Greek Ministry of Education (EPEAEK, Pythagoras I, 89206 RC AUTH 21914). Infrastructure funding provided by the Canada Foundation for Innovation (CFI) and Ontario Innovation Trust (OIT) is greatly acknowledged.

References

1 H. Meyer, F. Bosset, W. Vater and K. Stoepel, US Patent, 3799934 (1983).
2 A. Grunenberg, A. Hegasy, W. Mück, G. Franckowiak and R. R Kanikanti, Bayer AG, DOS 4130173 (1992).
3 A. Grunenberg, B. Keil and J. O. Heck, Int. J. Pharm., 118 (1995) 11.
4 A. Grunenberg, J. O. Henck and H. W. Siesler, Int. J. Pharm., 129 (1996) 147.
5 Nimodipine Monograph, European Pharmacopoeia 4th Ed.
6 T. M. Cardoso, P. O. Rodrigues, H. K. Stulzer, M. A. S. Silva and J. R. Matos, Drug Dev. Ind. Pharm., 31 (2005) 631.
7 D. Hörter and J. B. Dressman, Adv. Drug Deliv. Rev., 56 (2001) 75.
8 C. Leuner and J. Dressman, Eur. J. Pharm. Biopharm., 50 (2000) 47.
9 D. Q. M. Craig, Int. J. Pharm., 231 (2002) 131.
10 J. L. Ford, Pharm. Acta Helv., 61 (1986) 69.
11 S. Verheyen, N. Blaton, R. Kinget and G. Van den Mooter, Int. J. Pharm., 249 (2002) 45.
12 H. Suzuki and H. Sunada, Chem. Pharm. Bull., 46 (1998) 1015.
13 E. Sjokvist-Saers, C. Nystrom and M. Alden, Int. J. Pharm., 90 (1993) 105.
14 A. T. M. Serajudin, J. Pharm. Sci., 88 (1999) 1058.
15 B. C. Hancock and G. Zografi, J. Pharm. Sci., 86 (1997) 1.
16 D. Q. M. Craig, Thermochim. Acta, 248 (1995) 189.
17 H. E. Junginger and M. Wedler, Pharm. Res., 3 (1986) 41.
18 L. S. Taylor and G. Zografi, Pharm. Res.,15 (1998) 755.
19 K. L. A. Chan and S. G. Kazarian, Mol. Pharm., 1 (2004) 331.
20 J. Breitenbach, W. Schrof and J. Neumann, Pharm. Res., 16 (1999) 1109.
21 T. R. M. De Beer, W. R. C. Baeyens, Y. V. Heyden, J. P. Remon, C. Vervaet and F. Verpooort, Eur. J. Pharm. Sci., 30 (2007) 229.
22 S. G. Skoulika and C. Georgiou, Appl. Specrosc., 55 (2001) 1259.
23 S. G. Skoulika and C. Georgiou, Appl. Specrosc., 57 (2003) 407.
24 G. Z. Papageorgiou, D. Bikiaris, E. Karavas, S. Politis, A. Docoslis, P. Yong, A. Stergiou and E. Georgarakis, The AAPS J., 8 (2006) E623.
25 G. Fini, J. Raman Spectrosc., 35 (2004) 335.
26 N. A. Urbanetz and B. H. Lippold, Eur. J. Pharm. Biopharm., 59 (2005) 107.
27 G. M. M. Babu, C. D. S. Prasad and K. V. R. Murthy, Int. J. Pharm., 234 (2002) 1.
28 K. P. Chowdary, K. V. R. Murthy and C. H. D. S. Prasad, Indian Drugs, 32 (1995) 537.
29 J. W. Lu, M. Z. Wang, P. Ding and Z. S. Pan, Chin. Pharm. J., 30 (1995) 23.
30 F. Kopecky, B. Kopecka, P. Kaclik and D. Struharova, Ceska a Slovenska Farmacie, 47 (1998) 233.
31 J. Cucala, A. Garcia, M. Montes and R. Obach, Proc. Int. Symp. Control. Release Bioact. Mater., 21 (1994) 720.
32 N. A. Urbanetz, Eur. J. Pharm. Sci., 28 (2006) 67.
33 B. Bikiaris, G. Z. Papageorgiou, A. Stergiou, E. Pavlidou, E. Karavas, F. Kanaze and M. Georgarakis, Thermochim. Acta, 439 (2005) 58.
34 E. Karavas, E. Georgarakis and D. Bikiaris, Int. J. Pharm., 313 (2006) 189.
35 F. I. Kanaze, E. Kokkalou, I. Niopas, M. Georgarakis, A. Stergiou and D. Bikiaris, J. Appl. Polym. Sci., 102 (2006) 460.
36 P. Gupta and A. K. Bansal, AAPS Pharm. Sci. Tech., 6 (2005) E223.
37 P. Gupta, R. Thilagavathi, A. K. Chakraborti and A. K. Bansal, Mol. Pharm., 2 (2005) 384.
38 S. D. Wang, L. G. Herbette and D. G. Rhodes, Acta Crystalogr., C45 (1989) 1748.
39 F. I. Kanaze, E. Kokkalou, I. Niopas, M. Georgarakis, A. Stergiou and D. Bikiaris, J. Therm. Anal. Cal., 83 (2006) 283.
40 E. Karavas, E. Georgarakis and D. Bikiaris, J. Therm. Anal. Cal., 84 (2006) 125.
41 B. Barbas, R. Prohens and C. Puigjianer, J. Therm. Anal. Cal., 89 (2007) 687.
42 D. Kiss, R. Zelkó, Cs. Novák and Zs. Éhen, J. Therm. Anal. Cal., 84 (2006) 447.
43 C. Mao, S. C. Prasanth, S. R. Byrn and R. Pinal, Pharm. Res., 23 (2006) 2269.
44 T. Miyazaki, S. Yoshioka and Y. Aso, Chem. Pharm. Bull., 54 (2006) 1207.
45 R. Kalaiselvan, G. P. Mohanta, P. K. Manna and R. Manavalan, Pharmazie, 61 (2006) 618.
46 H. Konno and L. S. Taylor, J. Pharm. Sci., 95 (2006) 2692.
47 G. Fox, Bull. Am. Phys. Soc., 1 (1956) 123.
48 M. Gordon and J. S. Taylor, J. Appl. Chem., 2 (1962) 493.
49 Z. H. Ping, Q. T. Nguyen and J. Néel, Makromol. Chem., 189 (1988) 437.
50 J. Prinos, D. Bikiaris and C. Panayiotou, Polymer, 40 (1999) 4741.
51 E. Karavas, E. Georgarakis and D. Bikiaris, Eur. J. Pharm. Biopharm., 64 (2006) 115.
52 E. Karavas, E. Georgarakis, M. P. Sigalas, K. Avgoustakis and D. Bikiaris, Eur. J. Pharm. Biopharm., 66 (2007) 334.
53 E. Karavas, E. Georgarakis, A. Docoslis and D. Bikiaris, Int. J. Pharm., 340 (2007) 76.

Received: May 14, 2008
Accepted: July 24, 2008
OnlineFirst: November 12, 2008

DOI: 10.1007/s10973-008-9225-6